

Video Article

# Intra-lymph Node Injection of Biodegradable Polymer Particles

James I. Andorko<sup>\*1</sup>, Lisa H. Tostanoski<sup>\*1</sup>, Eduardo Solano<sup>1</sup>, Maryam Mukhamedova<sup>1</sup>, Christopher M. Jewell<sup>1</sup>

<sup>1</sup>Fischell Department of Bioengineering, University of Maryland, College Park

\*These authors contributed equally

Correspondence to: Christopher M. Jewell at [cmjewell@umd.edu](mailto:cmjewell@umd.edu)

URL: <https://www.jove.com/video/50984>

DOI: [doi:10.3791/50984](https://doi.org/10.3791/50984)

Keywords: Bioengineering, Issue 83, biomaterial, immunology, microparticle, nanoparticle, vaccine, adjuvant, lymph node, targeting, polymer

Date Published: 1/2/2014

Citation: Andorko, J.I., Tostanoski, L.H., Solano, E., Mukhamedova, M., Jewell, C.M. Intra-lymph Node Injection of Biodegradable Polymer Particles. *J. Vis. Exp.* (83), e50984, doi:10.3791/50984 (2014).

## Abstract

Generation of adaptive immune response relies on efficient drainage or trafficking of antigen to lymph nodes for processing and presentation of these foreign molecules to T and B lymphocytes. Lymph nodes have thus become critical targets for new vaccines and immunotherapies. A recent strategy for targeting these tissues is direct lymph node injection of soluble vaccine components, and clinical trials involving this technique have been promising. Several biomaterial strategies have also been investigated to improve lymph node targeting, for example, tuning particle size for optimal drainage of biomaterial vaccine particles. In this paper we present a new method that combines direct lymph node injection with biodegradable polymer particles that can be laden with antigen, adjuvant, or other vaccine components. In this method polymeric microparticles or nanoparticles are synthesized by a modified double emulsion protocol incorporating lipid stabilizers. Particle properties (e.g. size, cargo loading) are confirmed by laser diffraction and fluorescent microscopy, respectively. Mouse lymph nodes are then identified by peripheral injection of a nontoxic tracer dye that allows visualization of the target injection site and subsequent deposition of polymer particles in lymph nodes. This technique allows direct control over the doses and combinations of biomaterials and vaccine components delivered to lymph nodes and could be harnessed in the development of new biomaterial-based vaccines.

## Video Link

The video component of this article can be found at <https://www.jove.com/video/50984/>

## Introduction

The lymph nodes (LNs) are the command centers of the immune system. At this immunological site, antigen presenting cells prime naïve lymphocytes against specific foreign antigens to activate cellular and humoral immune responses. LNs have thus become an attractive target for delivery of vaccines and immunotherapies. Unfortunately, most vaccine strategies result in inefficient, transient delivery of antigen and adjuvants to the lymphoid tissue<sup>1</sup>. Approaches that improve the targeting and retention of vaccine components in LNs could therefore have a significant impact on the potency and efficiency of new vaccines.

One strategy for circumventing the challenge of LN targeting that has demonstrated great interest in new clinical trials is direct, intra-LN (*i.LN.*) injection<sup>2-4</sup>. These trials employed ultrasound guidance to deliver vaccines to LNs as a simple outpatient procedure. Compared to traditional peripheral injection routes, this approach resulted in significant dose-sparing and improved efficacy in therapeutic contexts including allergies and cancer<sup>2-4</sup>. These studies employed *i.LN.* injection of soluble vaccines (*i.e.* biomaterial-free) which were rapidly cleared by lymphatic drainage. Therefore, multiple injections- or cycles of multiple injections- were administered to achieve these impressive therapeutic effects. Improved retention in the LN could enhance the interaction between antigen and/or adjuvant and immune cells, further improving the potency of immune cell priming. This potential is supported by recent studies that show kinetics of antigen and adjuvant delivery play a critical role in determining the specific immune response generated<sup>5-7</sup>. Further, localizing and minimizing drug and vaccine doses could reduce or eliminate systemic effects, such as chronic inflammation.

Biomaterials have been studied extensively to enhance the potency and efficiency of vaccines<sup>1,8,9</sup>. Encapsulation in or adsorption on biomaterial carriers can physically shield cargo from degradation and overcome solubility limitations. Another notable feature of biomaterial carriers, such as polymeric micro- or nanoparticles, is the ability to coload several classes of cargo and, subsequently, release these cargos over controlled intervals. However, a significant limitation that continues to hinder biomaterial vaccines and immunotherapies *in vivo* is inefficient targeting of immune cells and limited trafficking to lymph nodes. For example, peripheral injection of biomaterial vaccines through conventional routes (e.g. intradermal, intramuscular) typically exhibit poor LN targeting, with up to 99% of the injected material remaining at the site of injection<sup>4,10</sup>. More recently, the size of biomaterial vaccine carriers has been tuned to improve preferential trafficking or drainage of these vaccines to LNs through interstitial flow<sup>8,10</sup>. These advances have led to enhanced cellular and humoral immune responses, underscoring the importance of targeting and engineering the LN environment for new vaccines.

This paper presents a vaccination protocol that combines lipid-stabilized polymer particles and *i.LN.* delivery to generate controlled release vaccine depots<sup>5,11</sup>. Building on recent studies employing surgical techniques for *i.LN.* in mice<sup>6,7,12,13</sup>, we developed a quick, nonsurgical strategy for injecting biomaterial vaccines in small animals<sup>5</sup>. Combining *i.LN.* delivery with biomaterial vaccine carriers potentially enhanced CD8 T cell

response within 7 days after a single injection of controlled release vaccine depots<sup>5</sup>. A strong humoral response (*i.e.* antibody titers) was also generated; both enhancements were linked to increased retention of vaccine components in lymph nodes that was mediated by controlled release from the biomaterial carriers. Interestingly, the size of vaccine particles altered the fate of these materials once in the LNs: nanoscale particles showed heightened direct uptake by cells, while larger microparticles remained in the extracellular LN environment and released cargo (*e.g.* adjuvant) that was taken up by LN-resident antigen presenting cells<sup>5</sup>. These data suggest two pathways that could be exploited for new vaccines by controlling the size of biomaterials injected *i.LN*.

In this article biodegradable lipid-stabilized polymer particles (micro- and nanoscale) are synthesized using a modified double emulsion strategy<sup>5,11</sup>. Particle properties are characterized by laser diffraction and microscopy. These particles are then injected directly into the inguinal LNs identified nonsurgically using a common, nontoxic tracer dye<sup>14</sup>. Post-injection analysis of LNs by histology or flow cytometry can be used to verify the distribution of particles within the LN environment, as well as to monitor cellular uptake and retention of particles over time. For protocols detailing histological processing and flow cytometry, readers are referred to recent JoVE articles and journal reports<sup>15-22</sup>. Typical results demonstrate local LN targeting of these depots that could be exploited to achieve potent, efficient immune responses or to tailor immunity for target pathogens.

## Protocol

All animal studies in this protocol were completed in compliance with Federal, State, and local guidelines, and using protocols reviewed and approved by the University of Maryland's Institutional Animal Care and Use Committee (IACUC).

## 1. Synthesis of Lipid-stabilized Micro- and Nanoparticles

1. In a 7 ml glass vial(s), combine DOPC, DSPE-PEG, and DOTAP lipids at a 60:20:20 molar ratio to prepare a master lipid mix.
  1. To synthesize a single sample: Transfer 242.9  $\mu$ l, 287.4  $\mu$ l, and 71.9  $\mu$ l, of DOPC, DSPE-PEG, and DOTAP respectively, into the vial using 2 ml glass serological pipettes.
  2. To synthesize multiple samples: Multiply each lipid volume above by the number of samples and combine into a single vial, then transfer equal aliquots of this lipid mixture into vials corresponding to each sample to be prepared.
  3. Dry lipids under a gentle stream of nitrogen gas for 10 min, or place in vacuum oven overnight.
2. In a single, empty 20 ml glass vial, dissolve 80 mg of PLGA in 5 ml of dichloromethane for each particle sample to generate a 16 mg/ml polymer stock solution.
3. Add 5 ml of polymer solution to the vial(s) containing the dried lipids, cap, and vortex for 30 sec.
4. To synthesize microparticles:
  1. Begin sonicating the organic phase containing the polymer, lipid, and other water-insoluble cargo on ice at 12 W using a sonicator.
  2. Create the water-in-oil (w/o) emulsion by using a pipette to add 500  $\mu$ l of distilled H<sub>2</sub>O, or H<sub>2</sub>O containing 1 mg of peptide, protein, or other water soluble cargo.
  3. Continue sonicating for 30 sec at 12 W on ice, gently rocking the vial up and down and side to side around the sonicator tip to ensure complete emulsification.
  4. Create the water-in-oil-in-water (w/o/w) emulsion by pouring the w/o emulsion into 40 ml of H<sub>2</sub>O in a 150 ml beaker.
  5. Homogenize for 3 min at 16,000 rpm using a digital homogenizer.
  6. Add a magnetic stir bar, transfer the beaker to a stir plate, and allow the w/o/w emulsion to stir overnight to remove the excess solvent.
5. To synthesize nanoparticles:
  1. Begin sonicating the organic phase containing the polymer, lipid, and other water insoluble cargo on ice at 14 W.
  2. Create the w/o emulsion by using a pipette to add 500  $\mu$ l of distilled H<sub>2</sub>O, or H<sub>2</sub>O containing 1 mg of peptide, protein, or other water soluble cargo.
  3. Continue sonicating for 30 sec at 14 W on ice.
  4. Create the w/o/w emulsion by pouring the w/o emulsion to 40 ml of H<sub>2</sub>O in a 150 ml beaker and sonicating for 5 min at 16 W on ice. Gently rock the vial up and down and side to side around the sonicator tip to ensure complete emulsification.
  5. Add a magnetic stir bar, transfer the flask to a stir plate and allow the w/o/w emulsion to stir overnight to remove the excess solvent.
6. The next morning, wash and collect particles:
  1. Pour emulsion through 40  $\mu$ m Nylon mesh cell strainer into a 50 ml conical tube.
  2. Centrifuge particles for 5 min at 5,000 x g for microparticles or 5 min at 24,000 x g for nanoparticles.
  3. Decant supernatant and wash particles by resuspending in 1 ml of H<sub>2</sub>O.
  4. Transfer suspended particles to a 1.5 ml microcentrifuge tube.
  5. Centrifuge for 5 min at 5,000 x g for microparticles or 5 min at 24,500 x g for nanoparticles.
  6. Wash particles twice more by removing supernatant, resuspending in 1 ml H<sub>2</sub>O, and centrifuging as in step 1.6.5. After washing, suspend particles in 1 ml H<sub>2</sub>O for immediate use, or lyophilize for extended storage.

## 2. Measurement of Synthesis Yield

1. Preweigh an empty 20 ml glass vial. Add 100  $\mu$ l of particle suspension to the preweighed vial after pipetting up and down with a micropipette to mix.
2. Lyophilize the particles or dry under a gentle stream of nitrogen.
3. Weigh the vial containing the dried polymer. Determine the particle yield in the vial by subtracting the original weight of the vial from the mass of the vial containing the dried particles.

4. Determine the overall particle yield by multiplying the particle mass in the vial by the dilution factor. To determine percent yield, divide the particle mass by the maximum theoretical input mass and multiply by 100%.

### 3. Determination of Particle Size

1. Clean the supplied cuvette-style glass fraction cell by filling with deionized water and wiping with cotton-tipped swab. Transfer 10 ml of distilled H<sub>2</sub>O to the cleaned fraction cell, add magnetic micro stir bar, and load the fraction cell into the cell mount of the particle size analyzer.
2. Adjust the magnetic stirring speed in the particle analyzer to achieve complete mixing in the fraction cell and close the compartment door.
3. Align the lasers to the fraction cell using the instrument software interface.
4. Use the instrument software interface to record a baseline reading with the fraction cell containing only distilled H<sub>2</sub>O.
5. Pipette the original particle suspension up and down with a micropipette to mix.
6. Pipette 10  $\mu$ l of particle suspension (typically approximately 0.5 mg) into the fraction cell. Ensure the volume of particle sample added to the cell is sufficient to generate signal strength in the appropriate range as indicated on the instrument software interface. The actual mass of particles required is dependent on percent yield and the optical properties of the particle sample.
7. Close the particle size analyzer compartment door and measure particle size using a refractive index of 1.60 for PLGA.
8. Use the software interface to calculate particle diameter using a number basis.

### 4. Visualization of Particles

1. Pipette particle suspension up and down with micropipette to mix. Dilute particle suspension to 1 mg/ml in deionized water.
2. Prepare a microscope slide by adding 3  $\mu$ l of diluted particle suspension and mounting a coverslip at a 45° angle to avoid bubble formation. Place the slide on microscope stage and image using the appropriate filter sets for each fluorescent cargo.

### 5. Preparation of Mice for *i.LN*. Injection

1. Prepare tracer dye solution:
  1. Prepare a 0.1% (w/v) solution of tracer dye by dissolving 10 mg of dye powder with 10 ml of distilled H<sub>2</sub>O.
  2. Sterilize the dye solution into a glass vial using a 0.2  $\mu$ m syringe filter.
2. One day prior to injection, anesthetize mouse using isoflurane according to an IACUC approved animal protocol. To evaluate depth of anesthesia, perform a toe pinch reflex test and monitor breathing rate to ensure a respiratory rate of approximately 100-140 breaths per minute.
3. Shave hair at base of tail and hindquarter using clippers while the mouse is anesthetized. Remove hair from the ventral side of the animal and laterally around to the dorsal side just above the joint of the hind leg (hip).
4. Inject tracer dye.
  1. For each dye injection, use a micropipette to transfer 10  $\mu$ l of dye solution into a microcentrifuge tube, and aspirate the entire 10  $\mu$ l into a 31G needle attached to a 1 ml syringe.
  2. Inject 10  $\mu$ l of dye solution subcutaneously on each side of the tail base where the hair was clipped, reloading in between injections.
5. Remove remaining hair by applying a mild depilatory cream via cotton swabs. Be sure to coat the area in between the hind thigh and abdomen.
6. Allow depilatory cream to incubate on skin for 3 min. After incubation, wet gloved hand with warm H<sub>2</sub>O and gently rub depilatory cream into skin.
7. Immediately remove depilatory cream by wetting gloved hand with warm H<sub>2</sub>O and rubbing tail base and hindquarter. Repeat until excess depilatory is removed, making sure to keep hand wet to avoid irritation.
8. Remove residual depilatory from mouse by wetting a soft cloth or paper towel with warm H<sub>2</sub>O and in a single motion, wiping lower portion of mouse. Avoid a rubbing motion to prevent abrasion or skin damage to the mouse.
9. Allow mouse to recover under a heat lamp and return to holding.

### 6. *i.LN*. Injection of Particles

1. On the following day, anesthetize mouse using isoflurane according to an IACUC approved animal protocol.
2. Examine the mouse to confirm drainage of tracer dye into each inguinal lymph node. The lymph node should be visible as a dark spot near the hind thigh and abdomen.
3. Prepare particle injection solution:
  1. Resuspend particles in distilled H<sub>2</sub>O at desired injection concentration. For each injection, use a micropipette to transfer 10  $\mu$ l of particle solution into a microcentrifuge tube.
  2. Aspirate the entire 10  $\mu$ l into a 31G insulin needle attached to a 1 ml syringe.
4. Inject particle dose:
  1. After visualizing LN, tighten skin around LN using thumb, index finger, and middle finger to pull skin taut and allow for controlled placement of the injection volume.
  2. Approach the LN with the needle at a 90° angle to the skin and penetrate the skin over the dyed LN to a depth of 1 mm.
  3. Slowly inject the entire volume. During injection, observe the LN volume through the skin to confirm injection by visible LN enlargement.
5. Allow the mouse to recover under a heat lamp and return to holding or conduct additional testing.

For relevant analysis techniques (e.g. histology, flow cytometry) see *JoVE* Articles 265, 1743, and 3054 and *Current Protocols in Immunology*, chapters 5 and 21<sup>15-22</sup>.

## Representative Results

Expected results for the protocols presented in this manuscript can be divided into three categories: particle synthesis, animal preparation, and particle injection.

**Figure 1** depicts the synthesis and characterization of biodegradable polymer particles, stabilized by amphiphilic lipids. Results of the emulsion/solvent evaporation synthesis protocol (**Figure 1A**) can be qualitatively assessed by visual inspection of the final emulsions generated; particle batches should be homogeneous, stable emulsions with an opaque appearance. Complications include emulsions that cream or flocculate, often due to improper storage of lipid stabilizers. To avoid this instability, lipids should be stored at -80 °C in a dehydrated state or in a sealed vial purged with nitrogen. Quantitative assessment of particle synthesis can be performed using laser diffraction or dynamic light scattering to analyze size distribution (**Figure 1B**). Expected results include tightly-distributed, monomodal particle sizes, indicating a uniform population of particles. The synthesis parameters described in this manuscript generate number averaged distributions centered at approximately 100 nm or 3 µm for nanoparticles and microparticles, respectively. Further qualitative assessment of particle synthesis can be achieved through modification of the above protocol to incorporate multiple classes of fluorescent cargo. In **Figure 1C**, microscopy images of microparticles loaded with a fluorescent peptide (FITC, green), a lipophilic dye (DiD, red), and an overlay image (yellow) confirm creation of particles within the desired size range and encapsulation of peptide within the volume of the particle.

The first two panels of **Figure 2** summarize the expected results of animal preparation for the *i.LN* injection strategy described in this paper. The methodology involves marking inguinal LNs by peripheral injection of a nontoxic tracer to identify the location for subsequent *i.LN* injection of particles (**Figure 2A**)<sup>5</sup>. As noted, drainage of the tracer dye following subcutaneous injection at the tail base will enable visualization of the inguinal LNs (**Figure 2B**)<sup>5</sup>. Ingestion of approved depilatory creams can pose hazards to the mice. Thus, care should be taken to thoroughly remove all cream applied, paying particular attention to paws, and the ventral side of the mice. Depilatory should be removed using a wet, soft cloth or wet paper towel in a single, smooth motion. Avoid rubbing to remove cream, as this can lead to abrasions on the exposed skin of the mice.

Confirmation of local of delivery to the inguinal LN can be evaluated through observation or histology. The LN volume can be monitored visually during injection as an indicator of successful injection. Expected results include efficient cargo distribution throughout the LN structure, without significant leakage to adjacent tissues or cells. Further, as injected fluid displaces/dilutes the tracer in the LN, dye concentration/coloring should become less intense after injection. Observation of the tissue should reveal an intact, but enlarged LN due to fluid injection. Potential challenges include injecting too rapidly or missing the LN, both of which can cause elution of the volume into surrounding subcutaneous tissue. These undesirable outcomes can be confirmed by necropsy or histology, where the particle suspension will be observed spreading to cells and tissue remote from nodes targeted for injection. In contrast, an expected result would be the identification of an enlarged inguinal LN due to containment of particles within the LN structure. Histological processing of excised LNs can definitively confirm delivery of cargo to the lymphoid tissue, as shown in **Figures 2C** and **2D**. Note that the particles in **Figure 2** incorporate fluorescent cargo to allow for visualization of cargo during injection, as well as during histological processing and fluorescent microscopy.

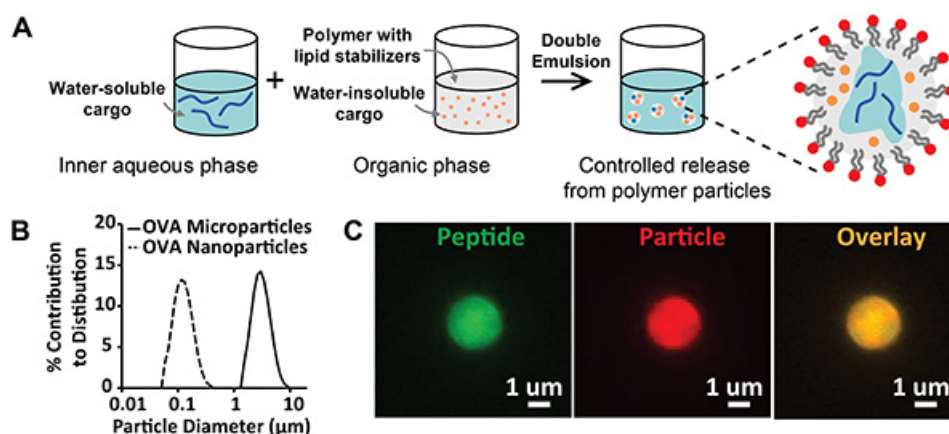


**Figure 1. Synthesis and Characterization of Lipid Stabilized Particles.** **A)** Schematic diagram describing the synthesis of lipid-stabilized particles prepared by emulsion/solvent evaporation. **B)** Size distributions of microparticles (solid line, diameter = 2.8 µm) and nanoparticles (dashed line, diameter = 113 nm). **C)** Fluorescent microscopy images of particles loaded with fluorescently-labeled peptide and a fluorescent particle dye. Labels: peptide (green) and particle (red). [Click here to view larger image.](#)



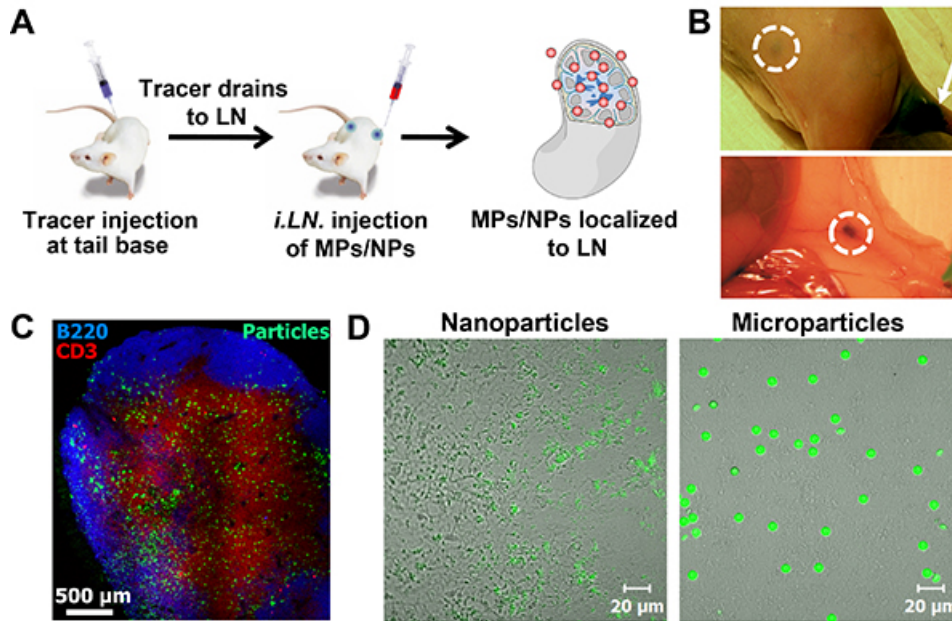


**Figure 2. *i.LN.* Injection and Distribution of Biodegradable Particles within LN.** **A)** Methodology for *i.LN.* injection. **B)** Visualization of LNs in a mouse through skin (upper image) and following necropsy (lower image)<sup>5</sup>. **C)** Histological staining of a LN confirming deposition and distribution of fluorescently-labeled polymer microparticles (particles, green; T-cells, red; B-cells, blue). **D)** Fluorescently-labeled nanoparticles (50 nm, left image) and microparticles (6  $\mu$ m, right image) in LNs 24 hr after injection. [Click here to view larger image.](#)

## Discussion

The technique described in this protocol allows controlled delivery of vaccines to LNs and to LN-resident antigen presenting cells. Biomaterial encapsulated cargo can be localized within the LN, enabling manipulation of the doses of one or more types of cargo delivered to the LN microenvironment. The localization and controlled release from polymer particles has been shown to generate a potent cellular and humoral immune response at significantly lower doses than conventional approaches. Further, through the manipulation of biomaterial carrier size, the primary mode of cellular processing can be modulated between direct uptake of nanoparticles or extracellular cargo release from larger microparticles<sup>5</sup>. These results establish the feasibility of *i.LN.* biomaterial delivery as a platform for therapeutic vaccine delivery.

The synthesis of PLGA particles by emulsion/solvent evaporation has been widely employed in drug delivery applications<sup>23,24</sup>. Thus potential challenges associated with this technique relate mostly to successful identification and deposition of vaccines in the LN target site. Although the use of tracer dye facilitates the visualization of the targeted inguinal LNs, the target size and depth beneath the skin are small. Thus, the authors recommend allotting time and mice for practicing the preparation and injections of mice. During animal preparation (*i.e.* shaving and application of depilatory), care should be taken not to cut the mice on the ventral side of the animal where the angle of the leg with the abdomen makes the skin more prone to injury from clippers. Additionally, all depilatory should be removed with warm water to prevent animals from ingesting the cream during normal grooming behavior. To practice LN injections, a higher tracer dye concentration can be administered and practice animals can be euthanized, and then injected multiple times. Following injection mice can be necropsied and the size of LNs from injected animals can be compared with an uninjected control LN. One limitation of this technique is the physical limit of the injection volume that can be loaded into the LN structure. Our protocol suggests an injection volume of 10  $\mu$ l in mice, though other studies have reported larger injection volumes at least as high as 20  $\mu$ l.<sup>13</sup> However, direct delivery of vaccines via *i.LN.* injection permits dramatic dose-sparing so the function of these vaccines should generally not be limited by volume constraints.

As noted, changing the physical property of the particles (*i.e.* size) is an effective mechanism to alter the pathway or outcomes induced by biomaterials and encapsulated cargos in LN tissue. The emulsion/solvent evaporation protocol can easily be modified to alter physical or chemical properties such as surface charge or functionality, and the rate of biodegradation/cargo release<sup>23,24</sup>. For example, the release kinetics can be tuned through alternative polymer compositions, and surface function can be altered using modified lipid compositions or poly(vinyl alcohol). The cargo loaded in particles can be easily manipulated to contain different antigens or adjuvants for target pathogens. The advantage of this approach is achieved through the combination of *i.LN.* delivery with local, controlled release of cargo from biomaterials. This synergy establishes a platform that can be exploited to efficiently generate adaptive immune responses using minute doses and with reduced nonspecific/systemic side effects.

## Disclosures

Production costs and access fees for this articles were partially sponsored by HORIBA, Ltd.

## Acknowledgements

This work was funded in part by the PhRMA foundation and a Research and Scholar Award from the University of Maryland, College Park. We thank Prof. Darrell Irvine for support of the initial work conducted in the completion of "*In situ* engineering of the lymph node microenvironment via intranodal injection of adjuvant-releasing polymer particles."<sup>5</sup>

## References

- Swartz, M. A., Hirose, S. & Hubbell, J. A. Engineering Approaches to Immunotherapy. *Sci. Transl. Med.* **4**, doi:10.1126/scitranslmed.3003763 (2012).
- Adamina, M. *et al.* Intranodal immunization with a vaccinia virus encoding multiple antigenic epitopes and costimulatory molecules in metastatic melanoma. *Mol. Ther.* **18**, 651-659, doi:10.1038/mt.2009.275 (2010).
- Ribas, A. *et al.* Intra-Lymph Node Prime-Boost Vaccination against Melan A and Tyrosinase for the Treatment of Metastatic Melanoma: Results of a Phase 1 Clinical Trial. *Clin. Cancer Res.* **17**, 2987-2996, doi:10.1158/1078-0432.ccr-10-3272 (2011).
- Senti, G. *et al.* Intralymphatic allergen administration renders specific immunotherapy faster and safer: a randomized controlled trial. *Proc. Natl. Acad. Sci. U.S.A.* **105**, 17908-17912, doi:10.1073/pnas.0803725105 (2008).
- Jewell, C. M., Lopez, S. C. B. & Irvine, D. J. *In situ* engineering of the lymph node microenvironment via intranodal injection of adjuvant-releasing polymer particles. *Proc. Natl. Acad. Sci. U.S.A.* **108**, 15745-15750, doi:10.1073/pnas.1105200108 (2011).
- Johansen, P. *et al.* Antigen kinetics determines immune reactivity. *Proc. Natl. Acad. Sci. U.S.A.* **105**, 5189-5194, doi:10.1073/pnas.0706296105 (2008).
- Randolph, G. J., Angeli, V. & Swartz, M. A. Dendritic-cell trafficking to lymph nodes through lymphatic vessels. *Nat. Rev. Immunol.* **5**, 617-628, doi:10.1038/nri1670 (2005).
- Irvine, D. J. & Jewell, C. M. in *Comprehensive Biomaterials*. eds Paul Ducheyne *et al.* Ch. 132 (2011).
- Moon, J. J., Huang, B. & Irvine, D. J. Engineering Nano- and Microparticles to Tune Immunity. *Adv. Mater.* **24**, 3724-3746, doi:10.1002/adma.201200446 (2012).
- Reddy, S. T. *et al.* Exploiting lymphatic transport and complement activation in nanoparticle vaccines. *Tissue Eng. Part A*. **14**, 734-735 (2008).
- Bershteyn, A. *et al.* Polymer-supported lipid shells, onions, and flowers. *Soft Matter*. **4**, 1787-1791, doi:10.1039/b804933e (2008).
- Johansen, P. *et al.* Direct intralymphatic injection of peptide vaccines enhances immunogenicity. *Eur. J. Immunol.* **35**, 568-574, doi:10.1002/eji.200425599 (2005).
- Mohanan, D. *et al.* Administration routes affect the quality of immune responses: A cross-sectional evaluation of particulate antigen-delivery systems. *J. Controlled Release*. **147**, 342-349, doi:10.1016/j.jconrel.2010.08.012 (2010).
- Harrell, M. I., Iritani, B. M. & Ruddell, A. Lymph node mapping in the mouse. *J. Immunol. Methods*. **332**, 170-174, doi:10.1016/j.jim.2007.11.012 (2008).
- He, H., Courtney, A. N., Wieder, E. & Sastry, K. J. Multicolor Flow Cytometry Analyses of Cellular Immune Response in Rhesus Macaques. *J. Vis. Exp.* e1743, doi:10.3791/1743 (2010).
- Matheu, M. P., Parker, I. & Cahalan, M. D. Dissection and 2-Photon Imaging of Peripheral Lymph Nodes in Mice. *J. Vis. Exp.* e265, doi:10.3791/265 (2007).
- Salmon, H. *et al.* Ex vivo Imaging of T Cells in Murine Lymph Node Slices with Widefield and Confocal Microscopes. *J. Vis. Exp.* e3054, doi:10.3791/3054 (2011).
- Donaldson, J. G. in *Current Protocols in Immunology: Immunofluorescence Staining*. John Wiley & Sons, Inc. (2001).
- Hofman, F. in *Current Protocols in Immunology: Immunohistochemistry*. John Wiley & Sons, Inc. (2001).
- Holmes, K., Lantz, L. M., Fowlkes, B. J., Schmid, I. & Giorgi, J. V. in *Current Protocols in Immunology: Preparation of Cells and Reagents for Flow Cytometry*. John Wiley & Sons, Inc. (2001).
- Sharrow, S. O. in *Current Protocols in Immunology: Overview of Flow Cytometry*. John Wiley & Sons, Inc. (2001).
- Sharrow, S. O. in *Current Protocols in Immunology: Analysis of Flow Cytometry Data*. John Wiley & Sons, Inc. (2001).
- Anderson, J. M. & Shive, M. S. Biodegradation and biocompatibility of PLA and PLGA microspheres. *Adv. Drug Deliv. Rev.* **28**, 5-24, doi:http://dx.doi.org/10.1016/S0169-409X(97)00048-3 (1997).
- Danhier, F. *et al.* PLGA-based nanoparticles: an overview of biomedical applications. *J. Controlled Release*. **161**, 505-522, doi:10.1016/j.jconrel.2012.01.043 (2012).